

Surface structure of a fluorinated thiol on Au(111) by scanning force microscopy

Makoto Motomatsu ^{a,*}, Wataru Mizutani ^b, Heng-Yong Nie ^b, Hiroshi Tokumoto ^b

^a Joint Research Centre for Atom Technology (JRCAT), Angstrom Technology Partnership (ATP), Higashi 1-1-4, Tsukuba, Ibaraki 305, Japan

^b Joint Research Centre for Atom Technology (JRCAT), National Institute for Advanced Interdisciplinary Research (NAIR), Higashi 1-1-4, Tsukuba, Ibaraki 305, Japan

Abstract

Scanning force microscopy (SFM) was used to study the surface structure of $\text{CF}_3\text{CF}_2(\text{CH}_2)_6\text{SH}$ (7,7,8,8,8-pentafluorooctanethiol, PFOT) monolayers self-assembled from a 1 mM trichloroethene (TCE) solution on Au(111). We observed many depressions with several to 20 nm diameters and 0.24 nm depth. In addition, especially around the step edges of Au, mounds 0.3–0.8 nm in height and with lower friction and higher stiffness than those of other regions were observed. These properties would result from the difference in the molecular orientation between on the mounds and on the flat parts. The molecular arrangement with the $(\sqrt{3} \times \sqrt{3}) R30^\circ$ structure was observed on the terraces of Au(111). By comparing the film thickness and the molecular length, the tilt angle of the molecular chain was found to be $56\text{--}76^\circ$ with respect to the surface normal. This large tilt angle allows the PFOT SAMs with the relatively large CF_3CF_2 -end group to pack closely on the $(\sqrt{3} \times \sqrt{3}) R30^\circ$ structure.

Keywords: Scanning force microscopy (SFM); Gold; Self-assembled monolayers; Molecular orientation; Self assembly

1. Introduction

Self-assembled monolayers (SAMs) [1] which are spontaneously adsorbed onto appropriate surfaces have high potential as the ultimate thin and well-ordered films. Among the SAMs, organomercaptanes on Au surfaces have been widely investigated using scanning probe microscopy [2,3], because of their excellent stability even in air and their atomically flat surfaces. Fluorine-terminated thiols are of great interest since fluorine atoms have inherent properties such as inertness to most chemical reagents, low friction coefficient and excellent repellency (practically nothing can stick to fluorine). These properties are essential for research and development of various surface modifiers or ultra thin resists [4].

In this paper we shall present the results on scanning force microscopy (SFM) of self-assembled $\text{CF}_3\text{CF}_2(\text{CH}_2)_6\text{SH}$ on Au(111) and discuss the effect of the relatively large diameter of the CF_3CF_2 -end group (ca. 0.56 nm [5], which is the estimated diameter of a perfluoromethylene chain in crystalline polytetrafluoroethylene) upon the molecular arrangement.

2. Experimental

PFOT (7,7,8,8,8-pentafluorooctanethiol: $\text{CF}_3\text{CF}_2(\text{CH}_2)_6\text{SH}$) was synthesized by thiolating the hydroxide group of $\text{CF}_3\text{CF}_2(\text{CH}_2)_6\text{OH}$. The composition was analyzed by NMR and its purity was confirmed to be better than 95.7% by a gas-chromatograph-mass-spectrometer.

Au(111) (thickness ca. 200 nm) films were evaporated on freshly cleaved mica surfaces in a vacuum deposition chamber [6,7]. The surface obtained was atomically flat with monoatomic steps. Onto this surface, we formed PFOT SAMs by immersion into a 1 mM trichloroethene (TCE) solution for 24 h. The surface was then rinsed with pure TCE to remove excess PFOT and dried with argon gas before measurements.

Contact angles against water, hexadecane and methylene iodide were measured by the free-standing drop method. SFM measurements were carried out using an AFM in a contact mode at 0.1 nN in air. A V-shaped microfabricated Si_3N_4 cantilever with a spring constant of 0.1 N m^{-1} was used. The local friction was measured using a 4-segment photodiode system [8]. For the local stiffness measurement, the sample was modulated along the z direction at 5 kHz with an amplitude of about 1 nm, and the cantilever response which reflects the local stiffness of the surface was measured with the lock-in technique [9,10].

* Corresponding author.

3. Results and discussion

Table 1 summarizes the results of contact angle measurements of an untreated Au(111) substrate, PFOT SAMs and a PTFE (polytetrafluoroethylene: $-(CF_2CF_2)_n-$, as a reference) film against water, hexadecane and methylene iodide. The surface free energies for these surfaces estimated using

Owens's equation [11] are also shown in this table. PFOT SAMs exhibited higher repellency than the untreated Au(111) substrate, leading to the low surface free energy which is one of the typical properties of fluorocarbon. Although contact angle data do not provide any information on surface structures, they indicate that the fluorine covers the surface macroscopically. The PFOT surface should show

Table 1

Contact angles against water, hexadecane and methylene iodide, together with calculated surface free energies (in this calculation, water surface energy of $72.8 \text{ dynes cm}^{-1}$ and methylene iodide surface energy of $50.8 \text{ dynes cm}^{-1}$ in [11] are used)

Surface	Contact angle (degrees)			Surface energy (dynes/cm)
	water	hexadecane	methylene iodide	
Untreated Au(111) substrate	80	<5	22	47.5
PFOT SAMs	104	28	60	28.7
PTFE film	112	43	78	20.1

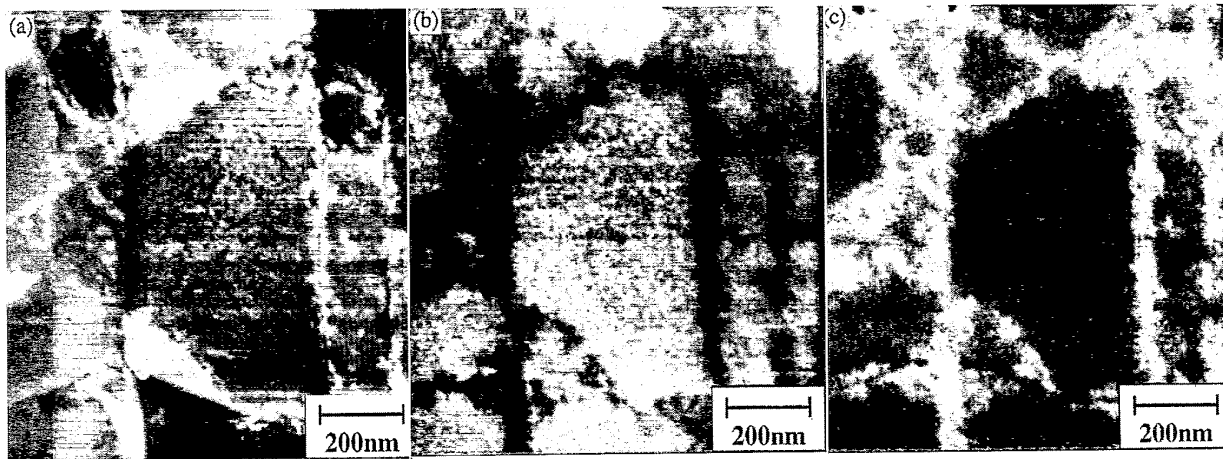


Fig. 1. Topography (a), friction (b) and stiffness (c) images of PFOT SAMs on Au(111). The bright areas in these images represent height in space, high friction and high stiffness, respectively. The mounds have lower friction and higher stiffness.

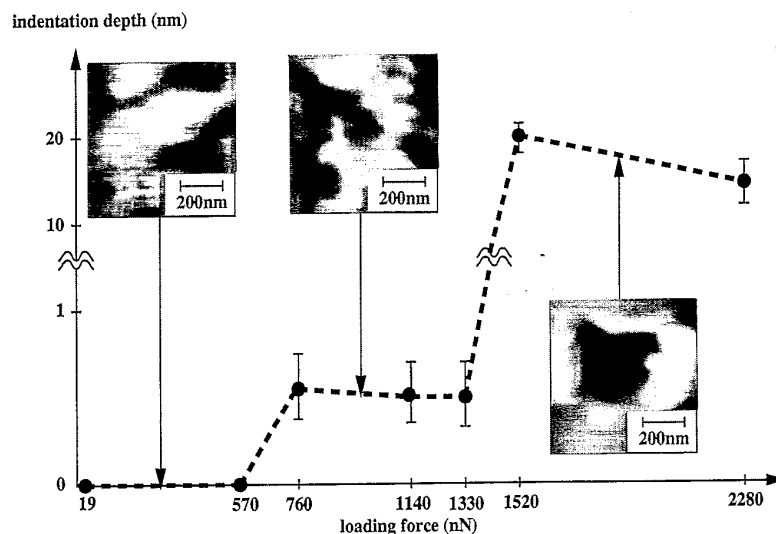


Fig. 2. Indentation depth versus loading force for PFOT SAMs on Au(111) together with AFM images after certain loading forces as indicated. The loading force (nN) is calculated as spring constant (19 N/m) \times cantilever deflection (nm).

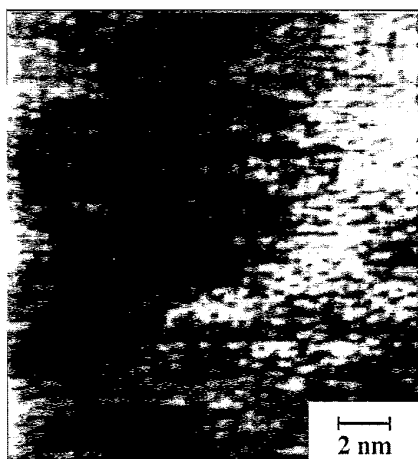


Fig. 3. High spatial resolution AFM topographic image of PFOT SAMs on Au(111).

a lower surface free energy than the PTFE film since the CF_3 group has lower surface tension than a CF_2 group. But this is not the present case. This can be explained by the fact that the effective contact area of rough surfaces (PTFE) is larger than that of flat surfaces (PFOT SAMs) and hence, according to Wenzel's equation [12], the roughness enhances the contact angle.

Fig. 1(a) shows an AFM topographic image of PFOT SAMs on Au(111) exhibiting many depressions with several to 20 nm diameters and about 0.24 nm depth on the terraces. Since the depth matches the Au single-atom step height, we can speculate that the depressions are formed as a result of etching of the Au surface by thiols during the PFOT adsorption process [2,13]. Most of the step edges of Au(111) are decorated with mounds 0.3–0.8 nm in height and several to 40 nm in width. These mounds are also found on the narrow terraces. Fig. 1(b) and Fig. 1(c) are the friction force and stiffness images of the same area as Fig. 1(a), respectively. The surface properties on the mounds are different from those on the flat parts; lower friction force and higher stiffness whose origin will be discussed later.

The thickness of the monolayer film was estimated by removing PFOT SAMs with an AFM tip. In the present exper-

iments, we scratched $200 \times 200 \text{ nm}^2$ areas at various applied loading forces by using a rectangular Si cantilever with a spring constant of 19 N m^{-1} . Fig. 2 shows the load–depth dependence for indentation of PFOT surfaces together with AFM images at certain loading forces. At 570 nN or less, no indentation occurred. However, between 760 nN and 1330 nN, the indentation depth was almost constant (0.33–0.76 nm). A typical square indentation region is seen in the centre of the inset image. At 1520 nN or more, the surface was damaged drastically. This large depth of the damage suggests that not only the PFOT SAMs but also the gold substrate was scratched due to the large loads. The thickness of PFOT SAMs, therefore, can be roughly estimated by the plateau indentation depth values of 0.33–0.76 nm. Using the PFOT molecular length of 1.37 nm, the tilt angle is calculated to be $56\text{--}76^\circ$ with respect to the surface normal, which is much larger than that of n-alkanethiols on Au [14]. This large tilt will be necessary to prevent the CF_3CF_2 - end groups directly touching each other in the direction of the tilt.

On the flat parts, we obtained the molecular image reproducibly as shown in Fig. 3, while such a molecular ordering was not obtained on the mounds. The molecular ordering shows the hexagonal symmetry which agrees with a $(\sqrt{3} \times \sqrt{3}) \text{ R}30^\circ$ structure on Au(111), where the nearest-neighbour spacing is $0.52 \pm 0.01 \text{ nm}$. However, the size of fluorocarbon chain (ca. 0.56 nm in diameter) is larger than the distance (ca. 0.50 nm) between the binding sites of the $(\sqrt{3} \times \sqrt{3}) \text{ R}30^\circ$ structure on Au(111). Therefore, on the flat parts, small stresses on the level surface of the position of the CF_3CF_2 - end group, except for the direction of the tilt, still exist leading to stress relaxation especially around the step edges. Fig. 4 is a schematic cross-sectional drawing of the molecular arrangement. Different orientations of the molecules may also result in the domain boundary around the step edges and in the narrow terraces where the molecules have smaller tilt angle. The area with less tilted molecules protrudes and has a higher density of fluorine than the other area, leading to lower friction since the fluorine atoms exhibit low friction [15]. It is also reasonable that the less tilted molecules show higher stiffness against the vertical force than the tilted molecules due to the orientation difference.

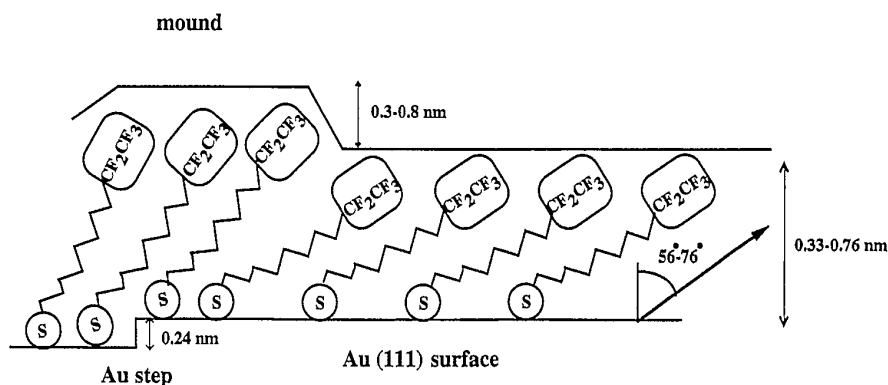


Fig. 4. A schematic cross-sectional structure of PFOT SAMs on Au(111).

4. Conclusion

We used SFM techniques to investigate the structure of PFOT SAMs on Au(111). The PFOT SAMs on Au(111) terraces formed the $(\sqrt{3} \times \sqrt{3})$ R30° structure, while especially around the step edges there were mounds whose surface exhibited lower friction and higher stiffness than those on the flat parts, probably due to the difference in the molecular orientation. The estimated tilt angle of 56–76° from the surface normal allows the PFOT SAMs with the relatively large CF₃CF₂- end group to arrange in the $(\sqrt{3} \times \sqrt{3})$ R30° structure on Au(111). The mounds will be formed to relax stresses caused by the larger size of the fluorocarbon chain than the distance between the binding sites of the $(\sqrt{3} \times \sqrt{3})$ R30° structure on Au(111).

Acknowledgements

This work was supported by the New Energy and Industrial Technology Development Organization (NEDO).

References

- [1] A. Ulman, *Introduction to Ultrathin Organic Films from Langmuir-Blodgett to Self-Assembly*, Academic Press, San Diego, 1991.
- [2] G.E. Poirier, M.J. Tarlov and H.E. Rushmeier, *Langmuir*, **10** (1994) 3383.
- [3] C.A. Alves, E.L. Smith and M.C. Porter, *J. Am. Chem. Soc.*, **114** (1992) 1222.
- [4] N. Mino, S. Ozaki, K. Ogawa and M. Hatada, *Thin Solid Films*, **243** (1994) 374.
- [5] C.E.D. Chidsey and D.N. Loiacono, *Langmuir*, **6** (1990) 682.
- [6] H.-Y. Nie, W. Mizutani and H. Tokumoto, *Surf. Sci.*, **311** (1994) L649.
- [7] W. Mizutani, A. Ohi, M. Motomatsu and H. Tokumoto, *Appl. Surf. Sci.*, **87/88** (1995) 398.
- [8] E. Meyer, R.M. Overney, D. Brodbeck, R. Lüthi, D. Brodbeck, L. Howald, H.J. Günterodt, O. Wolter, M. Fujihira, H. Takano and Y. Gotoh, *Thin Solid Films*, **220** (1992) 132.
- [9] M. Radmacher, R.W. Tillmann, M. Fritz and H.E. Gaub, *Science*, **257** (1992) 1900.
- [10] H.-Y. Nie, M. Motomatsu, W. Mizutani and H. Tokumoto, *J. Vac. Sci. and Technol. B*, **13** (1995) 1163.
- [11] D.K. Owens and R.C. Wendt, *J. Appl. Polymer Sci.*, **13** (1969) 1741.
- [12] R.W. Wenzel, *Ind. Eng. Chem.*, **28** (1936) 988.
- [13] C. Schönenberger, J.A.M. Sondag-Hunethorst, J. Jorritsma and L.G.J. Fokkink, *Langmuir*, **10** (1994) 611.
- [14] R.G. Nuzzo, L.H. Dubois and D.L. Allara, *J. Am. Chem. Soc.* **112** (1990) 558.
- [15] T. Kajiyama, K. Tanaka, I. Ohki, S.-R. Ge, J.-S. Yoon and A. Takahashi, *Macromolecules*, **27** (1994) 7932.